Hindawi
Advances in Civil Engineering
Volume 2022, Article ID 1040926, 9 pages
https://doi.org/10.1155/2022/1040926

Research Article

Study on the Damage Diagnosis of Ancient Wood Structure in Tianshui under Traffic Excitation

Xin Wang,[1] **Zhaobo Meng**,[2] **and Xicheng Zhang**[3]

[1]*School of Civil Engineering, Tianshui Normal University, Tianshui 741001, China*
[2]*School of Architecture & Civil Engineering, Liaocheng University, Liaocheng 252000, China*
[3]*School of Civil Engineering, Xi'an University of Architecture and Technology, Xi'an 710055, China*

Correspondence should be addressed to Xin Wang; wangxin@tsnu.edu.cn

Received 20 July 2022; Revised 27 September 2022; Accepted 30 September 2022; Published 4 November 2022

Academic Editor: Angelo Aloisio

Three-dimensional finite element model of the wood structure-foundation of the North House's main hall in Tianshui under ground traffic excitation was established, and the damage of the first-floor longitudinal beam of the wood structure was simulated by the finite element method. The node acceleration response signals on beams were decomposed with a wavelet packet. The wavelet packet energy curvature difference index was proposed to determine the structural damage location. The results show that the wavelet packet energy curvature difference can decide the damage location of the middle part of the first-floor longitudinal beam, and the index value increases with the increase of damage degree. If SNR is 40 db or larger, the damage index can accurately identify the damage of ancient wooden structures. When SNR increases, the damage index will have an increasingly higher sensitivity and certain ability to resist the effect of noise. The function relation between the damage index and the damage degree is obtained to determine the structural damage degree. The study results provide a theoretical basis for the damage diagnosis of the wood structure of ancient buildings along the traffic line.

1. Introduction

Tianshui is a historic city which boasts a large number of ancient architectures. Among others, Tianshui ancient dwellings were declared as one of the endangered heritage sites by The World Cultural Heritage Foundation in June 2005 [1]. Hu's ancient house is the representative of Tianshui Ming Dynasty houses, which is composed by North and South Houses. North House is grand, and its wood carving is unique. The North House's main hall building is the core part of the North House building with a unique design and magnificent atmosphere, which fully embodies the exquisite architectural art and profound cultural connotation of the Ming Dynasty. The plane of the main hall building is rectangular and faces south. The five rooms are 20.05 meters wide, the three rooms are 14.41 meters deep, and the height to the ridge is 11.4 meters. The plane of the North House's main hall in the courtyard is a double-eaved two-storied pavilion of hard hilltop brick and wood structure. Figure 1 is the front elevation of the main hall of the middle courtyard of the North House.

The main hall of the middle courtyard of the North House is located in MinZhu Road of QinZhou District Central Street in Tianshui city of GanSu province, only 20 meters away from the main road of the city traffic. The wood structure of the main hall building was seriously damaged in the WenChuan earthquake May 12th, 2008. With the development of urbanization in Tianshui, the number of ground traffic vehicles is increasing rapidly, and the continuous vibration of ground traffic makes structure fatigue damage and tenon and mortise loose, which threatens its safety. Therefore it is urgent to adopt effective technical means to repair and control structural damage.

Wavelet analysis has the functions of amplification, contraction, and shift. It can study the characteristics of signals by checking the changes under different magnifications. It has excellent time-frequency localization characteristics but has the disadvantage of poor resolution in high frequency band [2]. Wavelet packet analysis is an

Figure 1: Front elevation of the North House's main hall.

extension of the wavelet transform, which can provide a more refined analysis method for signals. The high frequency part of wavelet analysis without subdivision is further decomposed, and the corresponding frequency band is selected according to the characteristics of the analyzed signal to match the signal spectrum. Therefore, wavelet packet analysis was widely used in the field of damage diagnosis of civil engineering.

Since the 1980s, many scholars have engaged in the field of wavelet packets and achieved fruitful results. Ding et al. [3] adopted the wavelet packet energy spectrum method for structural damage early warning. Karami et al. [4] presented a method to identify the location of multiple damages in the piles of a dolphin pier, based on a combination of the Wavelet Packet Energy Curvature Difference (WPECD) and the richardson extrapolation. Angelo et al. [5] described the documentary and functional features of this peculiar antiseismic timber-based building technique. After a comparative analysis of the technique's features, the case of three T-F buildings, belonging to three different social classes is reported. Pan et al. [6] analyzed the acceleration response signal and identified the structural damage in real time with the wavelet packet energy spectrum. Lu et al. [7] extracted time-domain features and wavelet decomposition features of the parameters, and the patterns stored within each event were identified using the artificial neural network and support vector machine. Zhu et al. [8] simulated the damage of the beam in two working conditions, identified the damage with the wavelet packet energy curvature difference, and investigated the influence of the wavelet function and the number of decomposition layers on the recognition effect. Kankanamge et al. [9] described the latest application of wavelet transform in the health monitoring of civil engineering structures. Fan [10] established a finite element model of a wood frame and adopted a damage identification method combining the wavelet packet analysis method and stochastic resonance theory to evaluate the damage location and degree of the structure. Mei et al. [11] proposed a PQD detection method based on the wavelet packet transform (WPT) and improved complete ensemble empirical mode decomposition with adaptive noise (ICEEMDAN). Liu et al. [12] proposed the damage identification method of simply supported beam bridge based on wavelet analysis and coefficient of variation.

The damage of the first-floor longitudinal beam of the North House's main hall in Tianshui was simulated by finite element method under ground traffic excitation. The acceleration response signals of each node on the beam were decomposed by wavelet packet, and the damage location was studied by wavelet packet energy curvature difference. The index was sensitive to damage identification and can accurately determine the specific location of wood structure damage.

2. Wavelet Packet Analysis

Wavelet packet is composed of wavelet function, and i, j and k refer to its frequency, scale and shift parameters:

$$\psi_{j,k}^{i}(t) = 2^{j/2}\psi^{i}\left(2^{j}t - k\right), i = 1, 2, 3, \cdots. \tag{1}$$

The recursive relation of wavelet function ψ^{i} is

$$\begin{aligned} \psi^{2i}(t) &= \sqrt{2}\sum_{k=-\infty}^{\infty} h(k)\psi^{i}(2t-k), \\ \psi^{2i+1}(t) &= \sqrt{2}\sum_{k=-\infty}^{\infty} g(k)\psi^{i}(2t-k). \end{aligned} \tag{2}$$

where ψ is the wavelet generating function; $h(k)$ and $g(k)$ are the integral mirror filter coefficients, which are associated with the scaling function and the wavelet generating function.

j, $j+1$ order recursion formula are

$$f_{j}^{i}(t) = f_{j+1}^{2i-1}(t) + f_{j+1}^{2i}(t), \tag{3}$$

$$f_{j+1}^{2i-1}(t) = Hf_{j}^{i}(t), \tag{4}$$

$$f_{j+1}^{2i}(t) = Gf_{j}^{i}(t). \tag{5}$$

In the formula (4) and (5):

$$\begin{aligned} H\{\bullet\} &= \sum_{k=-\infty}^{\infty} h(k-2t), \\ G\{\bullet\} &= \sum_{k=-\infty}^{\infty} g(k-2t). \end{aligned} \tag{6}$$

H and G are filtering operators of expansion factor $h(k)$ and $g(k)$.

The initial signal $f(t)$ is

$$\begin{aligned} f(t) &= \sum_{i=0}^{2^{i}-1} f_{j}^{i}(t), \\ f_{j}^{i}(t) &= \sum_{k=-\infty}^{\infty} c_{j,k}^{i}(t)\psi_{j,k}^{i}(t), \\ c_{j,k}^{i}(t) &= \int_{-\infty}^{\infty} \psi_{j,k}^{i}(t)dt. \end{aligned} \tag{7}$$

3. Damage Diagnosis of Ancient Wood Structure

The damage diagnosis of ancient wood structure is divided into two parts: (1) the acceleration response signal of each node on the beam is decomposed by wavelet packet; (2) the energy

curvature difference of wavelet packet is calculated to locate and identify structural damage, including the selection of wavelet function and wavelet packet decomposition level.

3.1. Selection of Wavelet Function [13]. From the vanishing moment and support length, Daubechies wavelet (as well referred to dbN, N is Daubechies wavelet order) is selected. A larger N means a higher vanishing moment and a better time domain resolution. But the locality of time domain will become worse with the increase in the support length of Daubechies wavelet. Therefore, it is important to decide an appropriate order N of the Daubechies wavelet.

The structural dynamic response $f(N, K)$ is decomposed at a wavelet packet decomposition level of i, f_{ij} represents the structural response of the node (i, j), and the energy E_{ij} of the structure responds in each frequency band is [14]:

$$E_{ij} = \sum \left| f_{ij} \right|^2, \left(j = 0, 1, 2, \cdots, 2^i - 1 \right). \tag{8}$$

The wavelet packet energy spectrum E_i of the structural dynamic response $f(N, K)$ on the ith decomposition level can be expressed as follows:

$$E_i = \left\{ E_{i,j} \right\} = \left[E_{i0} \cdots E_{i1} \cdots E_{ij} \cdots E_{i2^i-1} \right]^T. \tag{9}$$

The cost function of each frequency band energy coefficient $\{E_{ij}\}$ on the ith decomposition level is defined to measure the good and bad of wavelet function. The norm entropy l^p is used as the cost function. On the same decomposition level of the wavelet packet, the cost function value of different wavelet functions is calculated and compared to decide an appropriate Daubechies order N. Usually, smaller is better regarding the cost function value calculated from different orders; The norm entropy l^p $(1 \le p \le 2)$ is defined as follows [14]:

$$S_L(E_i) = \sum_j \left| E_{i,j} \right|^p. \tag{10}$$

3.2. Selection of Wavelet Packet Decomposition Level [13]. Both the cost function and operation time are taken into consideration to decide the appropriate decomposition level of wavelet packet. In general, a smaller cost function means less operation time and better decomposition level of the wavelet packet. Similar to the selection of wavelet function order, the norm entropy l^p is used as the cost function to decide the appropriate decomposition level of wavelet packet, The norm entropy l^p $(1 \le p \le 2)$ is defined as follows [14]:

$$S_L(E_i) = \sum_j \left| E_{i,j} \right|^p. \tag{11}$$

3.3. Calculation Method of Curvature [8]. In practical engineering, the curvature is obtained from the second-order difference of the variable, namely, the rate of change of the slope, it is shown in Figure 2.

Its formula is

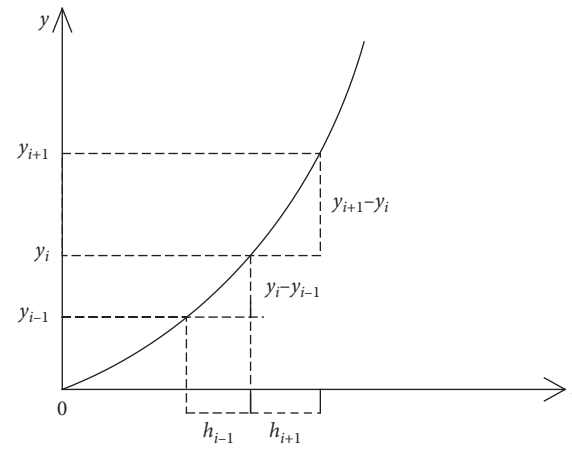

Figure 2: Diagram of curvature.

$$K_i = y_i^* = \frac{(y_{i+1} - y_i)/(h_{i+1}) - (y_i - y_{i-1})/(h_{i-1})}{(h_{i+1} + h_{i-1})/2}. \tag{12}$$

The numerator is the difference between the slope of the left and right node, and the denominator is the distance between the slope of the left and right node. If $h_{i-1} = h_{i+1}$, the curvature formula is expressed as follows:

$$K_i = y_i^* = \frac{(y_{i+1} - y_i)/(h) - (y_i - y_{i-1})/(h)}{h} = \frac{y_{i+1} - 2y_i + y_{i-1}}{h^2}. \tag{13}$$

Y is replaced by wavelet packet energy spectrum, and the energy curvature difference of the wavelet packet is

$$\Delta K_i = K_i^u - K_i^d. \tag{14}$$

k_i^u, k_i^d are the wavelet packet energy curvature of intact and damaged structures.

4. The Establishment of the Finite Element Model of the North House's Main hall

In the course of finite element simulation, firstly the beam-column nodes are established, and secondly the corresponding nodes are connected to build the beam-column elements. The wood beam and column are simulated with 3D elastic elements Beam188, which can withstand tension, compression and torsion, and each node has three translational degrees of freedom along x, y, and z direction and three reverse degrees of freedom around x, y, and z axis. Combin element 14 is used to simulate the mortise-and-tenon joints of beam-column. A mortise- and- tenon joint has three translational degrees of freedom (UX, UY, and UZ) and three reverse degrees of freedom (ROTX, ROTY, and ROTZ). The finite element overlapping nodes are established at the positions of the beam-column mortise and tenon joints. The spring element connects the column end node ① and the beam end node ②③④⑤, respectively. So the six spring elements are applied in the column and beam connection position to simulate the mortise-and-tenon joints are shown in Figure 3. The spring stiffness coefficient is

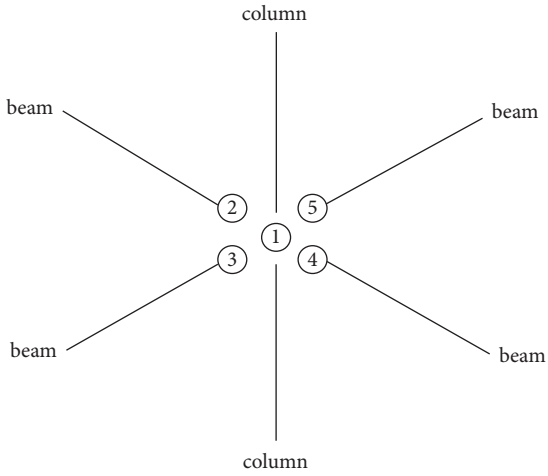

Figure 3: The simulation of the mortise-and-tenon joints of beam-column.

$K_x = 1.26 \times 10^9$ kN/m, $K_Y = K_z = 1.41 \times 10^9$ kN/m, $K_{\theta x} = K_{\theta y} = K_{\theta z} = 1.5 \times 10^{10}$ kN/m/rad [15].

The wood structure of the North House's main hall is measured by the research group. Because it has been built for a long time, no relevant measured material property index shows at present. With reference to the material parameters in literature [16, 17], the material parameters of wood and soil are shown in Table 1.

The large roof is simulated with Mass21, which has three translational degrees of freedom along x, y, and z direction and three reverse degrees of freedom around x, y, and z axis, and each direction has different mass and moment of inertia. Using the area equivalent method, the roof load is concentrated at the corresponding column ends, and obtain as $G = 1.925$ kN/m^2 [18].

According to the size of the wood structure of the main hall of the North House, the length, width, and depth of the foundation soil are 67.02, 39.25 and 8m respectively [19]. The foundation soil is simulated with Solid 45, which has three translational degrees of freedom along x, y and z direction and plasticity, creep, expansion, stress strengthening, large deformation, and large strain capabilities, and the length of the foundation soil unit is 2m. The corresponding node of the column heel and the foundation soil is coupled, and the system damping ratio is $\xi_i = \xi_j = 0.03$ [20].

Around the base and foundation soil with the method of fixed constraint, and the ground is free. The finite element model of the wood structure of the main hall and the foundation soil are shown in Figure 4~5.

5. Damage Diagnosis of the Wood Structure of the North House's Main hall

The main road in front of North House is four lanes, representative buses are selected to simulate the influence of traffic vehicles on the wood structure of the main hall. The vehicle speed of the city is low, so the speed of 40 km/h is selected to damage identification of the wood structure of the main hall. The vehicle load is applied vertically to the node of the lane unit, and the vehicle load is: $F(t) = 35000 + 8.64 \sin(6t)$, The time history curve and spectrum diagram are shown in Figure 6 [21], and the vehicle loading method is shown in Figure 7.

Table 1: Wood and soil parameters.

Materials	Thickness (m)	Elasticity modulus (MPa)	Density (kg/m^3)	Poisson ratio
Wood	—	8307	410	0.25
Foundation soil	8	11.2	1780	0.33

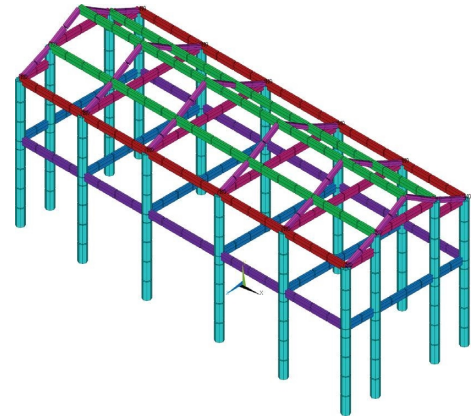

Figure 4: The FEM model of main hall wood structure of north house.

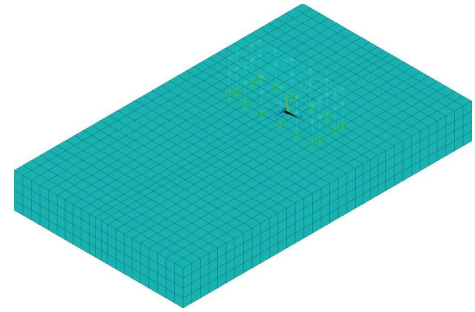

Figure 5: The FEM model of main hall wood structure of north house-foundation.

The midspan of longitudinal beam on the first floor of the upper timber structure is selected for damage diagnosis. The damage location and corresponding nodes are set as shown in Figure 8.

Damage can change the physical properties of the structure (mass, stiffness, and damping), it leads to change the modal characteristics of the structure (vibration frequency, mode shape and mode damping). The damage degree of the structure is represented by the reduction of the elastic modulus of the beam by 10% and 20% [14], and the damage Case 1 (ss10%) and the damage Case 2 (ss20%) are shown in Table 2.

5.1. The Selection of the Wavelet Function [13]. The vertical acceleration of midspan 134 node of the middle span beam on the first floor of the intact structure of the main hall is

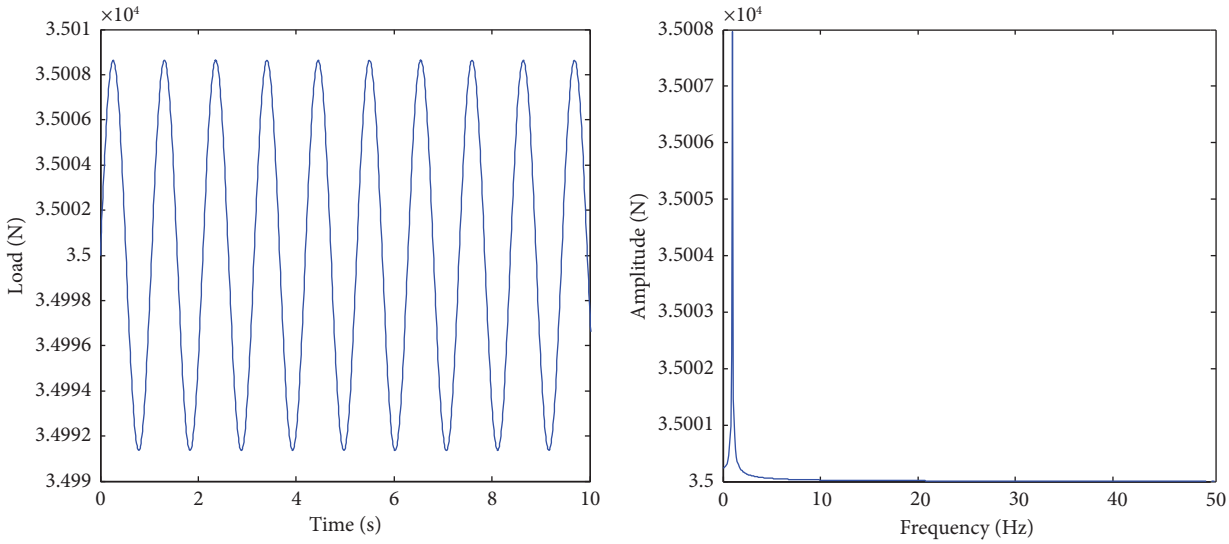

Figure 6: Time-history curve of vehicle load (a) and spectrogram (b).

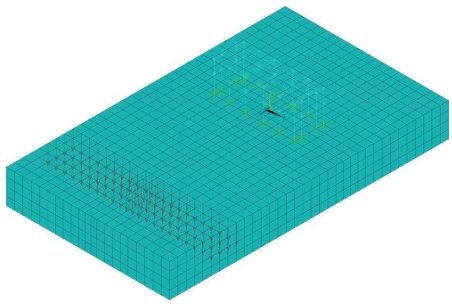

Figure 7: Vehicle loading mode.

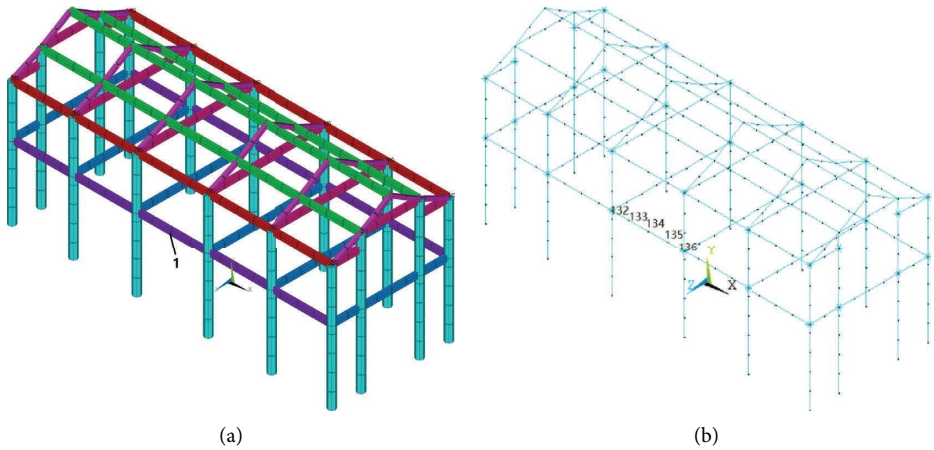

Figure 8: Damage position of wood beam (a) and corresponding nodes (b).

decomposed with wavelet packet Daubechies, and the decomposition is selected as 6 layers, the norm entropy is shown in Table 3. When N is 9, the norm entropy is minimum, so the Daubechies 9 is selected.

5.2. The Selection of the Decomposition Level [13]. The vertical acceleration of midspan 134 node of the middle span beam on the first floor of the intact structure of the main hall is decomposed with the wavelet Daubechies 9, and decompose

Table 2: Damage cases of wood structures.

Damage case	Damage position	Damage degree (%)	Remarks
1	Elements no. 162 and no. 163 (Corresponding nodes 133, 134, 135)	10	The mid-span of first-floor longitudinal beam
2	Elements no. 162 and no. 163 (Corresponding nodes 133, 134, 135)	20	The mid-span of first-floor longitudinal beam

Table 3: The cost function values for different wavelet orders.

Wavelet order N	6	7	8	9
$S_l(E_j)$ $(p = 1.5)$	$1.927e^5$	$1.916e^5$	$1.991e^5$	$1.389e^5$
wavelet order N	10	11	12	13
$S_l(E_j)$ $(p = 1.5)$	$1.516e^5$	$1.562e^5$	$1.663e^5$	$1.679e^5$
wavelet order N	14	15	16	17
$S_l(E_j)$ $(p = 1.5)$	$1.795e^5$	$1.834e^5$	$1.917e^5$	$1.952e^5$
wavelet order N	18	19	20	21
$S_l(E_j)$ $(p = 1.5)$	$2.087e^5$	$2.135e^5$	$2.280e^5$	$2.212e^5$

Table 4: The cost function values and computation time for different decomposition levels.

Decomposition level i	1	2	3	4
$S_l(E_j)$ $(p = 1.5)$	$9.881e^4$	$9.829e^4$	$9.775e^4$	$9.705e^4$
Operation time (s)	0.022	0.045	0.060	0.104
Decomposition level i	5	6	7	8
$S_l(E_j)$ $(p = 1.5)$	$9.576e^4$	$9.337e^4$	$8.849e^4$	$7.187e^4$
Operation time (s)	0.204	0.392	0.735	1.583

layers are 1–8. The norm entropy and time consumption are shown in Table 4. According to the time consumption, the decomposition level is set as 6.

5.3. Analysis of Wavelet Packet Energy Curvature Difference. The vertical acceleration of the beam node 132 to 136 of the main hall before and after the damage is decomposed with the wavelet Daubechies 9, and the decomposition level is 6. The energy curvature difference of the front eight wavelet packets and the corresponding nodes are taken as shown in Figure 9.

It could be seen from Figures 9(a)~9(h) that the energy curvature difference of the wavelet packet appears an obvious protrude at node 134, which is the same as the damage position of unit 162 and 163 under the damage Case 1 and 2 assumed above. Therefore, conclusion is drawn that the energy curvature of the wavelet packet can locate the damage of the structure.

5.4. The Analysis of the Sum of the front Eight Components of Wavelet Packet Energy Curvature Difference. The sum of the front eight components of wavelet packet energy curvature difference is taken as shown in Figure 10.

From Figures 10(a) and 10(b) the sum of the front eight components of wavelet packet energy curvature difference has an obvious protrusion at node 134, which is the same as the damage position 162 and 163 assumed above, and the distance to midspan is further, the damage index is smaller. Compared with wavelet packet energy curvature difference, the sum of the front eight components can better diagnose the damage location of the wood structure, and the damage degree increases and the index value increases.

5.5. Effect of Noise on Damage Diagnosis [13]. In the process of structural health monitoring, the signals collected from sensors are inevitably subject to the noise interference, generally assumed as Gaussian white noise. The original signals are overlaid with a value that is normally distributed and has a mean value of zero as the measurement noise. The level of signal noise is measured by the signal to noise ratio (SNR), which is defined as follows:

$$SNR = 10\log\left|\frac{\sum x^2(n)}{\sum y^2(n)}\right| = 20\log\frac{A_S}{A_N}\ (db), \tag{15}$$

where A_S is the root mean square of signal $x\ (n)$ and A_N is the root mean square of signal $y\ (n)$.

Here is the analysis of damage Case 1. To analyze how the white noise effect on the damage localization, Gaussian white noise with a SNR of 10 db, 20 db, 30 db, 40 db, and 50 db is added separately to the vertical acceleration response signal of each node on the beam in the intact structure and damaged structure. The wavelet packet is decomposed with Daubechies 9 and decomposition level 6. The sum of the front eight components of wavelet packet energy curvature difference under different noise levels is shown in Figure 11.

As can be seen from Figure 11, the damage index has a significant variation when SNR is 20 db or less, indicating that the damage index is greatly influenced by noise and is no longer able to identify the damage location. When SNR is 30 db, the damage index is less influenced by noise and could identify the damage. When SNR is 40 db or larger, the damage index is hardly influenced by noise and has a damage diagnosis ability similar to that under a noise-free condition. With the increase of SNR, the damage index will have an increasingly higher sensitivity to structural damage and certain ability to resist noise. If SNR is small, the damage index will be greatly influenced by noise, so the noise signal should be denoised as as possible to restore to the original.

5.6. The Analysis of Damage Degree. Assuming that the midspan of the first-floor longitudinal beam is damaged 10%~60%, the sum of the front eight components of the wavelet packet energy curvature difference at node 134 is defined as the damage index as shown in Table 5.

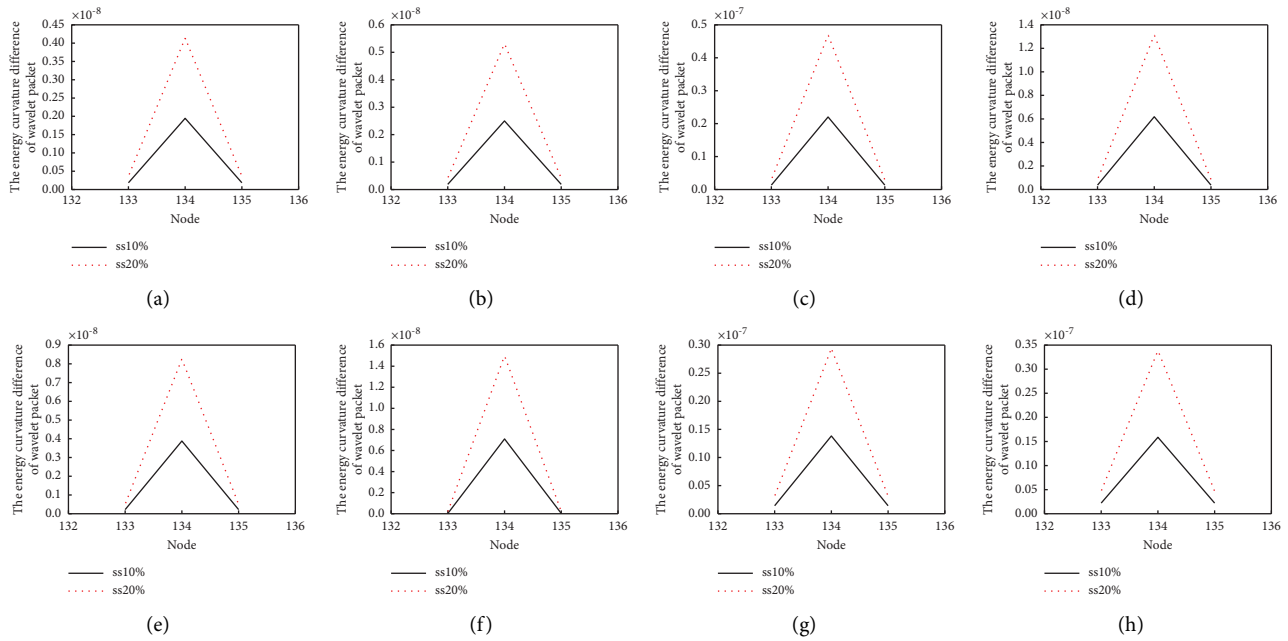

Figure 9: Wavelet packet energy curvature difference for damage cases 1 and 2.

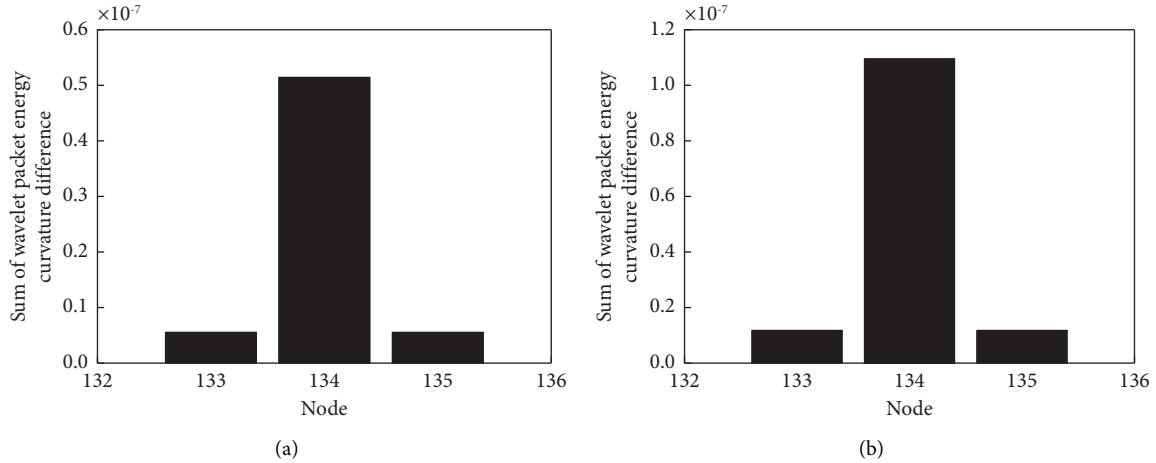

Figure 10: Sum of wavelet packet energy curvature difference for damage cases 1 and 2. (a) Damage cases 1. (b) Damage cases 2.

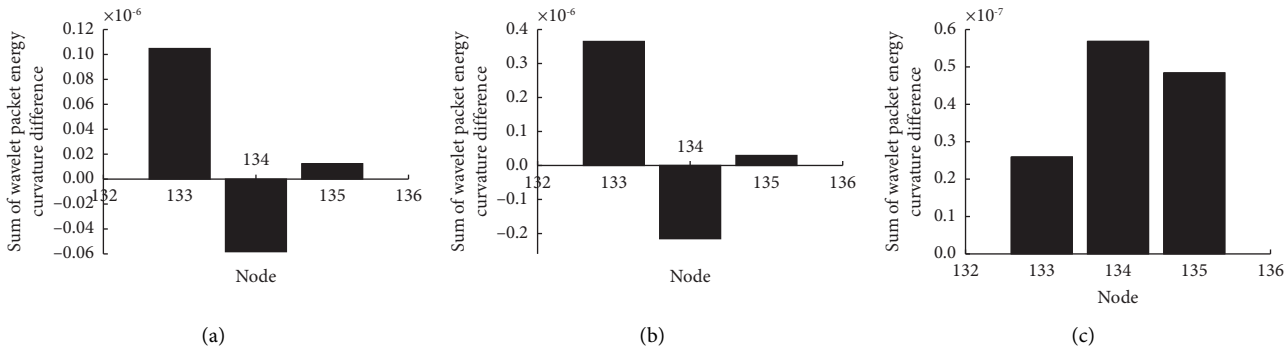

Figure 11: Continued.

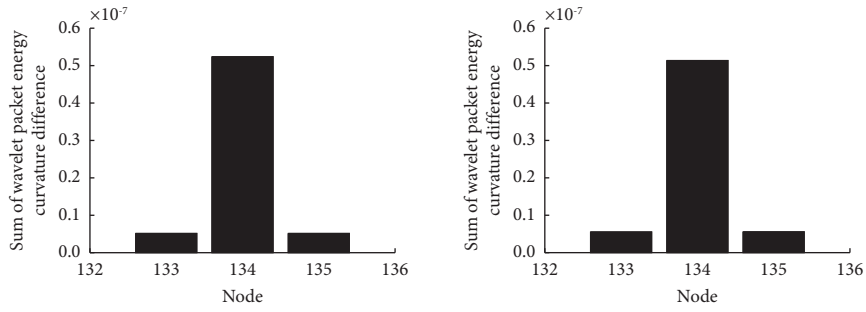

Figure 11: Sum of wavelet packet energy curvature difference under noise 10 db–50 db. (a) 10 db. (b) 20 db. (c) 30 db. (d) 40 db. (e) 50 db.

Table 5: Damage index.

Damage degree (%)	Damage index ($\times 10^{-7}$)
10	0.514
20	1.095
30	1.875
40	2.633
50	3.521
60	4.570

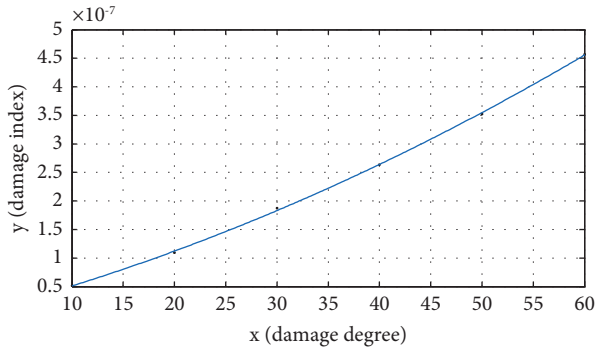

Figure 12: Relation of damage index and degree.

The relationship between the damage index and the damage degree at node 134 is obtained by using the numerical fitting of Matlab program as shown in Figure 12.

Based on Figure 12, the relationship between damage index and damage degree is obtained as follows. $Y = 0.000495X^2 + 0.04625X - 0.0016$. If y is obtained, x can be figured out from Figure 9.

6. Conclusion

The energy curvature difference of wavelet packet is proposed to damage location analysis for the longitudinal beam in the first floor of the wood structure of the main hall of the north house under ground traffic, and the conclusions are drawn as follows:

(1) Compared with the energy curvature difference of the wavelet packet, the localization effect of the sum of the front eight components is more obvious. When the damage degree increases, the index value increases.

(2) If SNR is 40 db or larger, the damage index can accurately identify the damage of ancient wood structures. When SNR increases, the damage index will have an increasingly higher sensitivity and certain ability to resist effect of noise.

(3) The relationship of the damage index and degree is developed by using Matlab program to judge the damage degree of the wood structure of the main hall of the North House, it will provide theoretical foundation for the damage diagnosis of the ancient wood structure under traffic excitation.

Data Availability

All data analyzed during this study are included in this article.

Conflicts of Interest

The authors declare that they have no conflicts of interest.

Acknowledgments

The work was supported by the National Natural Science Foundation of China (Grant no. 52068063), Gansu Province Natural Science Foundation Research Program (Grant no. 21JR1RE286), Gansu Province Higher Education Innovation Fund Project (Grant no. 2020B-173), Fuxi Scientific Research Innovation Team Project (Grant no. FXD2020-13), Maijishan Grottoes Art Research Project of Tianshui Normal University (Grant no. MJS2021-06), Shandong Province Natural Science Foundation Research Program (Grant no. ZR2020ME240), and Natural Science Basic Research Program of Shaanxi (Grant no. 2022JM-223).

References

[1] T. Sun, "The reflection to the status and conservation of Tianshui historical residences," *Modern Urban Studies*, vol. 11, pp. 20–25, 2008.

[2] Y. Fu-sheng, *Engineering Analysis and Application of Wavelet Transform*Science Press, Beijing, China, 2001.

[3] Y.-liang Ding, Li Ai-qun, and Y. Deng, "Parameters for identification of wavelet packet energy spectrum for structural damage alarming," *Journal of Southeast University (Natural Science Edition)*, vol. 41, no. 4, pp. 824–828, 2011.

[4] V. Karami, M. R. Chenaghlou, and A. M. Gharabaghi, "A combination of wavelet packet energy curvature difference and Richardson extrapolation for structural damage detection," *Applied Ocean Research*, vol. 101, no. 8, Article ID 102224, 2020.

[5] A. Aloisio, M. Fragiacomo, and G D'Alo, "The 18th-cba," *International Journal of Architectural Heritage*, vol. 14, no. 6, pp. 870–884, 2020.

[6] Y. Pan, L. Zhang, X. Wu, K. Zhang, and M. J. Skibniewski, "Structural health monitoring and assessment using wavelet packet energy spectrum," *Safety Science*, vol. 120pp. 652–665, C, 2019.

[7] Y.Ju Lu and C. H. Wang, "Integration of wavelet decomposition and artificial neural network for failure prognosis of reciprocating compressors," *Process Safety Progress*, vol. 40, no. 3, pp. 105–115, 2021.

[8] Yu Zhu, He Xia, and J. M. Goicolea, "Experimental study on bridge damage identification based on wavelet packet energy curvature difference method," *Journal of Vibration and Shock*, vol. 32, no. 5, pp. 20–25, 2013.

[9] Y. Kankanamge, Y. Hu, and X. Shao, "Application of wavelet transform in structural health monitoring," *Earthquake Engineering and Engineering Vibration*, vol. 19, no. 2, pp. 515–532, 2020.

[10] J. X. Fan, *Research on the Structural Damage Identification Method Based on Stochastic Resonance Dissertation*, Xi'an University of Architecture and Technology, Xi'an, China, 2018.

[11] Yu Mei, Y. Wang, X. Zhang, S. Liu, Q. Wei, and Z. Dou, "Wavelet packet transform and improved complete ensemble empirical mode decomposition with adaptive noise based power quality disturbance detection," *Journal of Power Electronics*, vol. 22, no. 8, pp. 1334–1346, 2022.

[12] L. Guang-yao, Xi-jun Liu, and S. Zhang, "Damage identification of simply supported beam bridge based on wavelet analysis and variation coefficient," *Chinese Journal of Applied Mechanics*, vol. 37, no. 5, pp. 1915–1922, 2020.

[13] X. Wang, W. Bing Hu, and Z. Bo Meng, "Damage alarming analysis for ancient wood structures based on wavelet packet energy spectrum," *Multidiscipline Modeling in Materials and Structures*, vol. 10, no. 4, pp. 593–610, 2014.

[14] Li Ai-qun and Y.-liang Ding, *The Theory and Application of Engineering Structural Damage Alarming*, Science Press, Beijing, China, 2007.

[15] F. Dong-ping, Yu Mao-hong, and Y. Miyamoto, "Numerical analysis on structural characteristics of ancient timber architecture," *Engineering Mechanics*, vol. 18, no. 1, pp. 137–144, 2001.

[16] M. Zhao-bo, *Analysis and Assessment of the Vibration Responds Traffic-Induced of Xi'an bell tower*, Xi'an University of Architecture and Technology, Xi'an, China, 2009.

[17] Institute of Mechanical Industry Investigation and Design, *Engineering Geological Survey Report of Xi'an bell tower*, Institute of Mechanical Industry Investigation and Design, Xi'an, China, 1985.

[18] Da-feng Gao, Z. Song-tao, and X. J Ding, "Analysis of structural and seismic performance of yongning gate embrasured watchtower of xi'an city wall," *Journal of Shandong University*, vol. 43, no. 2, pp. 62–69, 2013.

[19] M. Y. Qiu and Y. Ya-nan, "Analysis of influence depth for roads induced by vehicle loadz," *Rock and Soil Mechanics*, vol. 31, no. 6, pp. 1822–1826, 2010.

[20] X.-ming Yuan, R. Sun, and J. Sun, "Laboratory experimental study on dynamic shear modulus ratio and damping ratio of soils," *Earthquake Engineering and Engineering Vibration*, vol. 20, no. 4, pp. 133–139, 2000.

[21] Z.-chuang Liang, *The Dynamic Response Analysis of Xi'an City Wall Structure under Traffic Random Loads*, Xi'an University of Architecture and Technology, Xi'an, China, 2013.